MODELLING STRAIN INDUCED MARTENSITE FORMATION DURING FORMING

Lars-Erik Lindgren[*]

[*] Department of Applied Physics and Mechanical Engineering
Luleå University of Technology, 971 87 Luleå, Sweden
e-mail: Lars-Erik.Lindgren@ltu.se, web page: http://www.ltu.se

Key words: Plasticity, Strain induced martensite, Parameter determination.

Summary. *The Olson-Cohen model for strain-induced martensite formation is combined with a mixture rule for material properties in order to create a material model that can be used in simulations forming of components made of HyTensX™. The model cannot capture the effect of plastic strain at higher temperatures on martensite formation during later straining at lower temperatures. However, the model is expected to work well for common forming processes.*

1 INTRODUCTION

Martensite can form during forming operation of metastable austenitic stainless steels. This changes the material properties significantly and must therefore be included in the constitutive model when simulating forming processes. Modelling this phenomenon requires a model for martensite formation coupled to a constitutive model. The Olson-Cohen model[1] was applied for a AISI301 type material in Reference 2. The temperature range is extended in this work. Stress, martensite content and the temperature are logged in tensile tests and compared with the predictions of the model. It is found that the model also handles the reduced formation of martensite formation at higher temperatures well. Tests with prestrain above the temperature range for martensite formation has been performed and shows that it has an influence on subsequent martensite formation at lower temperatures, which the Olson-Cohen model can not capture.

2 STRAIN INDUCED MARTENSITE FORMATION AND MIXTURE RULES

The current work focuses on strain induced martensite formation (SIMT). Olson and Cohen[1] proposed a physical based model for SIMT where shear band intersections has a probability to be nuclei for martensite formation. Stringfellow *et al.*[3] extended this model by including stress into the probability function. Tanaka and Iwamoto[4] further developed the model.

It is assumed that only two phases coexist in the material. They are austenite (γ) and α'-martensite (M). It is only necessary to compute the martensite fraction. The evolution equation for the martensite formation becomes

$$\dot{X}_M = \left(1 - X_M\right)\left(A_M \dot{\bar{\varepsilon}}_\gamma + B_M \dot{g}\right) \tag{1}$$

$$A_M = A_{sb}\xi\eta n X_{sb}^{n-1}\left(1 - X_{sb}\right) \tag{2}$$

$$B_M = \eta X_{sb}^n \frac{d\xi}{dg} H\left(\dot{g}\right) \tag{3}$$

$$\dot{g} = -\dot{T} + g_1 \dot{K}_\sigma \tag{4}$$

Where the shear band fraction X_{sb} in Eq. (2) is obtained from the plastic strain rate in austenite as

$$\dot{X}_{sb} = A_{sb}\left(1 - X_{sb}\right)\dot{\bar{\varepsilon}}_{\gamma} \tag{5}$$

The factor A_{sb} is written as

$$A_{sb} = \left(A_1 T^2 + A_2 T + A_3 - A_4 K_{\sigma}\right)\left(\frac{\dot{\bar{\varepsilon}}_{\gamma}}{\dot{\bar{\varepsilon}}_{ref}}\right)^M \tag{6}$$

The notations and equations are explained in detail in References 2 and 5. The last term in Eq. (1) is the effect of the change in probability of martensite formed at shear band intersections and is ignored. The parameters were determined as described in Reference 2 and are given in Table 1 for HyTensX, a metastable austenitic stainless steel. However, the rate dependency factor in Eq. (6) could not be determined from those experiments and is thus excluded from the table. Simple mixture rules are used to compute the elastic modulus, thermal expansion and plastic properties. Data for Young's modulus for austenite and martensite versus temperature were obtained from Tomita & Shibutani[6] and the thermal dilatation from Iwamoto. Tomita and Iwamoto[4] proposed a model for the flow stress of the phases. They used

$$\sigma_y^{\gamma} = C_4^{\gamma} e^{-C_5^{\gamma} T} + C_1^{\gamma}\left[1 - e^{-C_2^{\gamma}\bar{\varepsilon}_{\gamma}^p}\right]^{C_3^{\gamma}} \tag{6}$$

for austenite and

$$\sigma_y^M = C_4^M e^{-C_5^M T} + C_1^M\left[1 - e^{-C_2^M \bar{\varepsilon}_M^p}\right]^{C_3^M} \tag{7}$$

The yield stress of the mixture of two phases is computed by

$$\sigma_y = \left(1 - X_M\right)\sigma_y^{\gamma}\left(\bar{\varepsilon}_{\gamma}^p\right) + X_M \sigma_y^M\left(\bar{\varepsilon}_M^p\right) \tag{17}$$

The plastic properties determined in 2 and given in the table below. The distribution of the plastic strain between the two phases is obtained by assuming

$$\sigma_y^{\gamma} d\bar{\varepsilon}_{\gamma}^p = \sigma_y^M d\bar{\varepsilon}_M^p \tag{18}$$

$$d\bar{\varepsilon}^p = X_y d\bar{\varepsilon}_{\gamma}^p + X_M d\bar{\varepsilon}_M^p \tag{19}$$

A_1	A_2	A_3	A_4	σ_g	g_0	g_1	η	n
$-3.9 \cdot 10^{-4}$	$2.7 \cdot 10^{-2}$	56.9	7.15	65.8	-182	67.7	11.1	4.5

Table 1. Martensite formation parameters for HyTensX.

C_1^{γ}	C_2^{γ}	C_3^{γ}	C_4^{γ}	C_5^{γ}	C_1^M	C_2^M	C_3^M	C_4^M	C_5^M
998	0.82	0.66	1673	0.0058	1701	15.74	4.25	7733	0.0148

Table 2. Yield limit parameters for HyTensX from 2

3   NUMERICAL ISSUES OF STRAIN-STRESS ALGORITHM

The previous model causes large complications in the strain-stress logic as the thermal dilatation and even Young's modulus depend on the plastic strain via the strain-induced phase change. The logic for a strain-stress algorithm is given in Reference 5.

4   RESULTS

Six tensile testes were performed. The time, temperature, true strain, true stress and martensite fraction were obtained from the measurements. The time, strain and temperatures were used to drive the algorithm for computing martensite formation and stress. Figure 1a shows a comparison between measured and computed martensite fraction for the different tests. Figure 1b shows the same for the stresses.

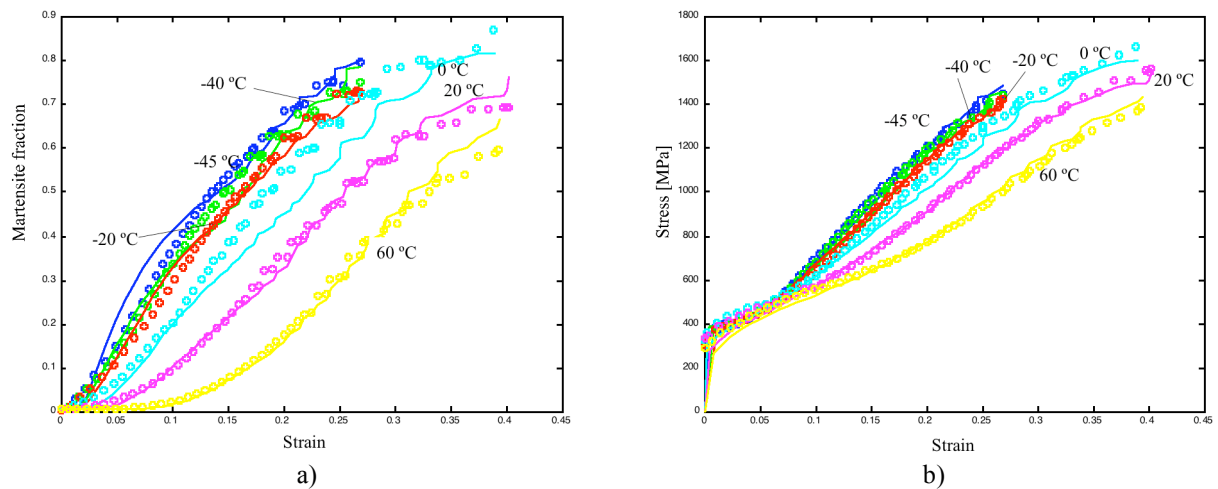a)   b)

Figure 1. Measured and computed martensite fractions a) and stress b) for the different tests identified by their approximate initial temperature.

Three different tests were performed where the test specimens were heated to about 90°C, well above the temperature where martensite can be formed by straining. They were elongated by 5, 10 and 15%, respectively. Thereafter they were cooled to 25°C at which tensile tests were performed as in the previous chapter. The figure shows the measured martensite fraction versus strain. Temperatures were logged also. The smaller difference between 10% and 15% prestrain than between 10% and 5% prestrain is probably due to a larger temperature increase during the test of the sample with 15% restrain due to problem to control the temperature. The strain is the total strain, i.e. the strain during the low temperature test plus the prestrain at the higher temperature.

The model in Eq.s (1-6) accounts only for the current strain rate and has no dependency on previously accumulated plastic strain on the martensite formation. The result below shows that this effect is noticeable. The previous plastic straining can become active nuclei for martensite formation during later deformation stages also.
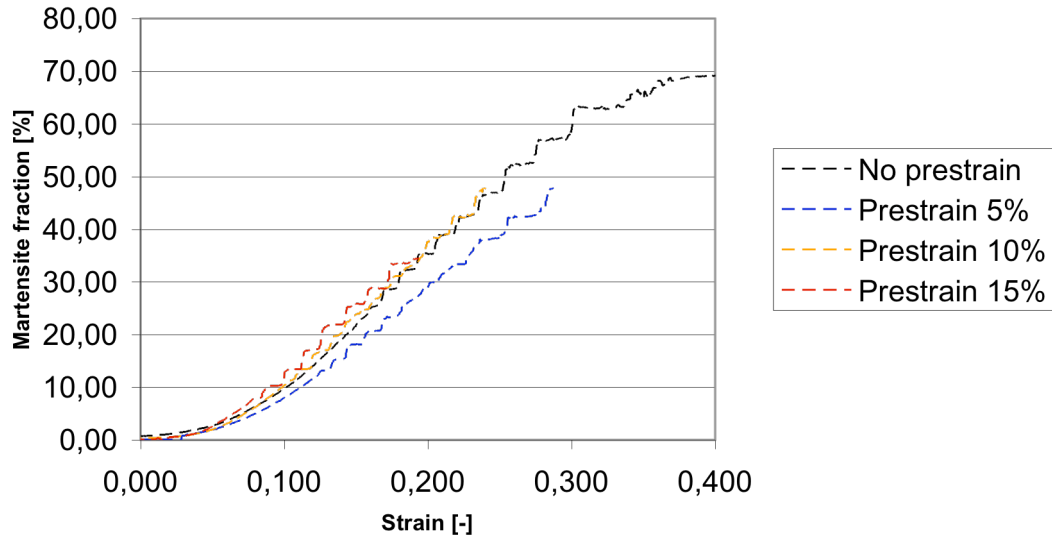
Figure 2. Effect of prestraining on martensite formation.

12 CONCLUSIONS

- The Olson-Cohen model together with the mixture rules works well for the tensile tests where strain-induced martensite forms.
- The model does cannot include the effect of prestraining at higher temperatures on later deformation. It is only the current plastic strain rate that has a probability to cause martensite formation.

13 ACKNOWLEDGEMENTS

REFERENCES

[1] G. Olson and M. Cohen, Kinetics of strain-induced martensitic nucleation. *Metallurgical Transacations A*, **6A**(April), 791-795 (1982).

[2] L.-E. Lindgren. Models for forming simulations of metastable austenitic stainless steel. in *8th International Conference on Numerical in Industrial Forming Processes, NUMIFORM '04*, Ohio, USA (2004).

[3] R. Stringfellow, D. Parks, and G. Olson, A constitutive model for transformation plasticity accompanying strain-induced martensitic transformation in metastable austenitic steels. *Acta Metallurgical*, **40**(7), 1703-1716 (1992).

[4] T. Iwamoto and T. Tsuta, Computational simulation of the dependence of the austenitic grain size on the deformation behavior of TRIP steels. *International Journal of Plasticity*, **16**(7-8), 791-804, (2000).

[5] K. Domkin and L.-E. Lindgren, Return mapping strain-stress algorithm extended to strain induced martensite formation, submitted for publication.

[6] Y. Tomita and Y. Shibutani, Estimation of deformation behavior of TRIP steels -- smooth/ringed-notched specimens under monotonic and cyclic loading. *International Journal of Plasticity*, **16**(7-8), 769-789 (2000).